



ELSEVIER

Contents lists available at ScienceDirect

Comptes Rendus Chimie

www.sciencedirect.com



Preliminary communication/Communication

# Fluorine and chlorine doping in oxygen-deficient perovskites: A strategy for improving chemical stability



Nataliia Tarasova\*, Irina Animitsa

Ural Federal University, Institute of Natural Sciences and Mathematics, Russia

## ARTICLE INFO

## Article history:

Received 21 March 2019

Accepted 2 May 2019

Available online 31 May 2019

## Keywords:

Perovskite

Anionic doping

Fluorine doping

Chlorine doping

Proton conductors

Chemical stability

## ABSTRACT

The present work describes the effect of fluorine and chlorine doping on the chemical stability of proton conductors  $\text{Ba}_2\text{In}_2\text{O}_5$ ,  $\text{Ba}_4\text{In}_2\text{Zr}_2\text{O}_{11}$ , and  $\text{Ba}_4\text{Ca}_2\text{Nb}_2\text{O}_{11}$  against carbon dioxide and water steam. It was proved that both undoped and halide-doped compositions demonstrate good chemical stability under  $\text{H}_2\text{O}$  treatment without degradation and without any hydrolytic decomposition. The hydration process leads to the change in the crystal structure only. The treatment in the  $\text{CO}_2/\text{air}$  (1:1) atmosphere (500 °C, 10 h) leads to the decomposition of undoped samples only. Halide-doped samples retain their structure without detectable products, that is, they are more chemically stable compared with undoped compositions. The method of halide doping can be used as the promising technique for obtaining the new perovskite-related materials with high level of chemical stability.

© 2019 Académie des sciences. Published by Elsevier Masson SAS. All rights reserved.

## 1. Introduction

Perovskite-related complex oxides with high level of ionic conductivity can be used as electrolytic materials of solid oxide fuel cells. However, the operating temperatures of these fuel cells (900–1000 °C) are very high; and the search of alternative materials with lower working temperatures is very important. The use of proton-conducting complex oxides has a several advantages [1–8], such as a decrease in operating temperatures (500–700 °C) and an increase in the efficiency.

The poor chemical stability in the atmosphere of carbon dioxide and water vapor is the limiting factor for application of the protonic electrolytes as the components of solid oxide fuel cells [9]. A compromise between high proton conductivity and chemical stability must be found to create long-term working electrochemical devices based on solid oxide protonic conductors.

The novel strategy for simultaneously improving transport properties and chemical stability is the method of the

anionic doping of perovskite-related matrix. The halide-doped ( $\text{F}^-$ ,  $\text{Cl}^-$ , and  $\text{Br}^-$ ) barium cerate  $\text{BaCeO}_3$  demonstrates the good chemical stability against  $\text{CO}_2$  and  $\text{H}_2\text{O}$  steam [10,11]. At the same time, the introduction of small amount of  $\text{F}^-$  and  $\text{Cl}^-$  ions in the oxygen sublattice of proton conductors  $\text{Ba}_2\text{In}_2\text{O}_5$ ,  $\text{Ba}_4\text{In}_2\text{Zr}_2\text{O}_{11}$ , and  $\text{Ba}_4\text{Ca}_2\text{Nb}_2\text{O}_{11}$  leads to the increase in oxygen ion and proton conductivity [12–15]. However, the investigation of chemical stability against  $\text{CO}_2$  and  $\text{H}_2\text{O}$  steam for these halide-doped compounds was not carried out. Earlier it was proved that In-contained compounds are not favorable for using for industrial applications because of the presence of In, reducing stability of complex oxides [4]. In this work, the compositions with different types of the structures  $\text{Ba}_2\text{In}_2\text{O}_5$ ,  $\text{Ba}_4\text{In}_2\text{Zr}_2\text{O}_{11}$ , and  $\text{Ba}_4\text{Ca}_2\text{Nb}_2\text{O}_{11}$  (brownmillerite, ordinary, and double perovskites) were chosen to establish the fundamental regularities of the effect of anion doping on chemical stability of proton conductors.

## 2. Experimental section

The samples  $\text{Ba}_2\text{In}_2\text{O}_5$ ,  $\text{Ba}_4\text{In}_2\text{Zr}_2\text{O}_{11}$ ,  $\text{Ba}_4\text{Ca}_2\text{Nb}_2\text{O}_{11}$ ,  $\text{Ba}_2\text{In}_2\text{O}_{4.95}\text{F}_{0.1}$ ,  $\text{Ba}_4\text{In}_2\text{Zr}_2\text{O}_{10.95}\text{F}_{0.1}$ ,  $\text{Ba}_4\text{Ca}_2\text{Nb}_2\text{O}_{10.95}\text{F}_{0.1}$ ,

\* Corresponding author.

E-mail address: [Natalia.Tarasova@urfu.ru](mailto:Natalia.Tarasova@urfu.ru) (N. Tarasova).

$\text{Ba}_2\text{In}_2\text{O}_{4.95}\text{Cl}_{0.1}$ ,  $\text{Ba}_4\text{In}_2\text{Zr}_2\text{O}_{10.95}\text{Cl}_{0.1}$ , and  $\text{Ba}_4\text{Ca}_2\text{Nb}_2\text{O}_{10.95}\text{Cl}_{0.1}$  were prepared by a solid state method from preliminary dried stoichiometric amounts of high-purity powders  $\text{BaCO}_3$ ,  $\text{CaCO}_3$ ,  $\text{In}_2\text{O}_3$ ,  $\text{ZrO}_2$ ,  $\text{Nb}_2\text{O}_5$ ,  $\text{BaCl}_2$ . Before weighing, the starting materials were dried. The stoichiometric mixtures were mixed in agate mortar and then calcined (800, 900, 1000, 1100, 1200, and 1300 °C) with regrindings after each stage.

The X-ray powder diffraction (XRD) measurements were made using a Bruker Advance D8 diffractometer with Cu  $K\alpha$  radiation. The crystal structures of anhydrous and hydrated samples were determined through Rietveld refinement using FULLPROF software.

Thermogravimetric analysis was carried out using a simultaneous thermal analyzer 409 PC analyzer (Netzsch) coupled with a quadrupole mass spectrometer QMS 403 C Aëolos (Netzsch). For the preparation of hydrated forms of the specimens the powder samples were hydrated at slow cooling from 900 to 200 °C (1 °C/min) under a flow of wet nitrogen. The “wet” nitrogen was obtained by bubbling the  $\text{N}_2$  at room temperature first through distilled water and then through saturated solution of KBr ( $p_{\text{H}_2\text{O}} = 2 \times 10^{-2}$  atm). The cooling was performed to a temperature not lower than 200 °C to avoid the appearance of adsorbed water.

The  $\text{CO}_2$  stability of samples was determined on the anhydrous powders that were exposed to the  $\text{CO}_2/\text{air}$  (1:1) mixture at 500 °C for 10 hours. The treated powders were then examined by XRD.

### 3. Results and discussions

#### 3.1. X-ray characterization

All halide-doped samples are single phase and they are isostructural to their parent compositions. Brownmillerite-type phases  $\text{Ba}_2\text{In}_2\text{O}_{4.95}\text{X}_{0.1}$  (hereinafter  $\text{X} = \text{F}^-$ ,  $\text{Cl}^-$ ) are characterized by the space group  $Ibm2$ ; perovskites  $\text{Ba}_4\text{In}_2\text{Zr}_2\text{O}_{10.95}\text{X}_{0.1}$  have the space group  $Pm\bar{3}m$ ; and double perovskites  $\text{Ba}_4\text{Ca}_2\text{Nb}_2\text{O}_{10.95}\text{X}_{0.1}$  have the space group  $Fm\bar{3}m$ . It should be noted that the X-ray data for all investigated parent compositions, all fluorine-doped compositions, and chlorine-doped sample  $\text{Ba}_4\text{Ca}_2\text{Nb}_2\text{O}_{10.95}\text{Cl}_{0.1}$  are in good agreement with the previously reported data [12–16]. The data for the samples  $\text{Ba}_2\text{In}_2\text{O}_{4.95}\text{Cl}_{0.1}$  and  $\text{Ba}_4\text{In}_2\text{Zr}_2\text{O}_{10.95}\text{Cl}_{0.1}$  are obtained for the first time in this work.

As can be seen in Table 1, the introduction of ions with smaller radius ( $\text{F}^-$ ) in the oxygen sublattice leads to the decrease in the cell parameters, and the introduction of ions with larger radius ( $\text{Cl}^-$ ) leads to the increase in the cell parameters ( $r_{\text{O}^{2-}}$ ,  $r_{\text{F}^-}$ , and  $r_{\text{Cl}^-} = 1.81 \text{ \AA}$  [17]).

**Table 1**

Cell volume of anhydrous samples.

Sample	$V(\text{\AA}^3)$	Sample	$V(\text{\AA}^3)$	Sample	$V(\text{\AA}^3)$
$\text{Ba}_2\text{In}_2\text{O}_5$	607.90	$\text{Ba}_4\text{In}_2\text{Zr}_2\text{O}_{11}$	74.30	$\text{Ba}_4\text{Ca}_2\text{Nb}_2\text{O}_{11}$	602.28
$\text{Ba}_2\text{In}_2\text{O}_{4.95}\text{F}_{0.1}$	604.18	$\text{Ba}_4\text{In}_2\text{Zr}_2\text{O}_{10.95}\text{F}_{0.1}$	74.25	$\text{Ba}_4\text{Ca}_2\text{Nb}_2\text{O}_{10.95}\text{F}_{0.1}$	601.85
$\text{Ba}_2\text{In}_2\text{O}_{4.95}\text{Cl}_{0.1}$	608.09	$\text{Ba}_4\text{In}_2\text{Zr}_2\text{O}_{10.95}\text{Cl}_{0.1}$	74.35	$\text{Ba}_4\text{Ca}_2\text{Nb}_2\text{O}_{10.95}\text{Cl}_{0.1}$	603.15

#### 3.2. Treatment under water vapor pressure ( $p_{\text{H}_2\text{O}} = 2 \times 10^{-2}$ atm)

The capability for reversible water uptake from the gas phase for undoped  $\text{Ba}_2\text{In}_2\text{O}_5$  [18],  $\text{Ba}_4\text{In}_2\text{Zr}_2\text{O}_{11}$  [19],  $\text{Ba}_4\text{Ca}_2\text{Nb}_2\text{O}_{11}$  [20], all fluorine-doped [14,21], and chlorine-doped  $\text{Ba}_4\text{Ca}_2\text{Nb}_2\text{O}_{10.95}\text{Cl}_{0.1}$  [13] samples was described earlier. It was proved that anionic doping ( $\text{F}^-$ ,  $\text{Cl}^-$ ) leads to the decrease in the degree of hydration with the increase in the concentration of halide ions. Thermal and mass spectrometric (MS) studies for  $\text{Ba}_2\text{In}_2\text{O}_{4.95}\text{Cl}_{0.1}$  and  $\text{Ba}_4\text{In}_2\text{Zr}_2\text{O}_{10.95}\text{Cl}_{0.1}$  were carried out in the present work (Fig. 1). As can be seen, the mass loss was observed at the temperature range 300–400 °C. This process was accompanied by an intense endothermic effect on the differential scanning calorimetry (DSC) curve. The MS analysis indicated that the mass changes are the result of water loss; no other volatile compounds ( $\text{CO}_2$ ,  $\text{O}_2$ , or  $\text{HCl}$ ) were detected. It should be noted that the thermal and MS results for  $\text{Ba}_2\text{In}_2\text{O}_{4.95}\text{Cl}_{0.1}$  and  $\text{Ba}_4\text{In}_2\text{Zr}_2\text{O}_{10.95}\text{Cl}_{0.1}$  were similar to the results for other halide-doped compounds based on  $\text{Ba}_2\text{In}_2\text{O}_5$ ,  $\text{Ba}_4\text{In}_2\text{Zr}_2\text{O}_{11}$ , and  $\text{Ba}_4\text{Ca}_2\text{Nb}_2\text{O}_{11}$ .

The hydration process leads to the changes in the crystal structure of hydrated samples compared with anhydrous samples. Halide-doped samples based on brownmillerite  $\text{Ba}_2\text{In}_2\text{O}_5$  transform to the tetragonal structure similar to  $\text{Ba}_2\text{In}_2\text{O}_5 \cdot n\text{H}_2\text{O}$  (space group  $P4/mmm$ ). The hydrated undoped  $\text{Ba}_4\text{In}_2\text{Zr}_2\text{O}_{11} \cdot n\text{H}_2\text{O}$  and halide-doped  $\text{Ba}_4\text{In}_2\text{Zr}_2\text{O}_{10.95}\text{X}_{0.1} \cdot n\text{H}_2\text{O}$  samples belong to the  $P4_2/n$  space group. The hydration of double perovskite  $\text{Ba}_4\text{Ca}_2\text{Nb}_2\text{O}_{11}$  leads to the appearance of monoclinic distortions, and hydrated composition  $\text{Ba}_4\text{Ca}_2\text{Nb}_2\text{O}_{11} \cdot n\text{H}_2\text{O}$  belongs to  $P2_1/n$  space group. The hydrated halide-doped  $\text{Ba}_4\text{Ca}_2\text{Nb}_2\text{O}_{10.95}\text{X}_{0.1} \cdot n\text{H}_2\text{O}$  samples belong to the  $P4_2/n$  space group. It should be noted that values of cell volumes for hydrated chlorine-doped samples were obtained for the first time. The hydration of samples leads to the lattice expansion for both undoped and doped samples in comparison with anhydrous samples (Table 2). The X-ray data for sample  $\text{Ba}_4\text{Ca}_2\text{Nb}_2\text{O}_{10.95}\text{Cl}_{0.1} \cdot n\text{H}_2\text{O}$  are presented in Fig. 2.

Therefore, both undoped  $\text{Ba}_2\text{In}_2\text{O}_5$ ,  $\text{Ba}_4\text{In}_2\text{Zr}_2\text{O}_{11}$ , and  $\text{Ba}_4\text{Ca}_2\text{Nb}_2\text{O}_{11}$  and halide-doped  $\text{Ba}_2\text{In}_2\text{O}_{4.95}\text{X}_{0.1}$ ,  $\text{Ba}_4\text{In}_2\text{Zr}_2\text{O}_{10.95}\text{X}_{0.1}$ , and  $\text{Ba}_4\text{Ca}_2\text{Nb}_2\text{O}_{10.95}\text{X}_{0.1}$  samples demonstrate good chemical stability under  $\text{H}_2\text{O}$  treatment without degradation and without any hydrolytic decomposition. The hydration process leads to the change in the crystal structure only.

#### 3.3. Treatment under carbon dioxide atmosphere

The investigation of the chemical stability of undoped and halide-doped samples under  $\text{CO}_2$  treatment was

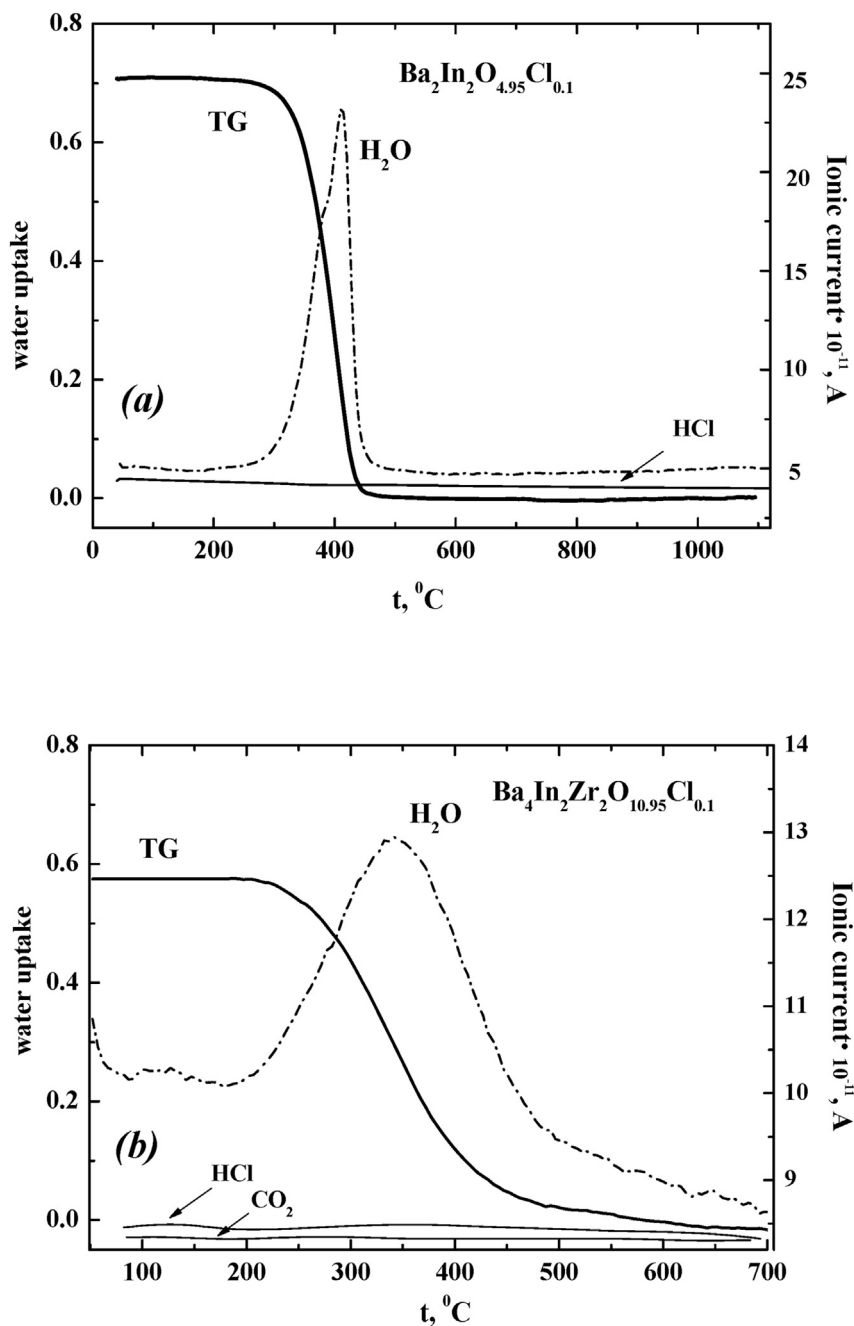
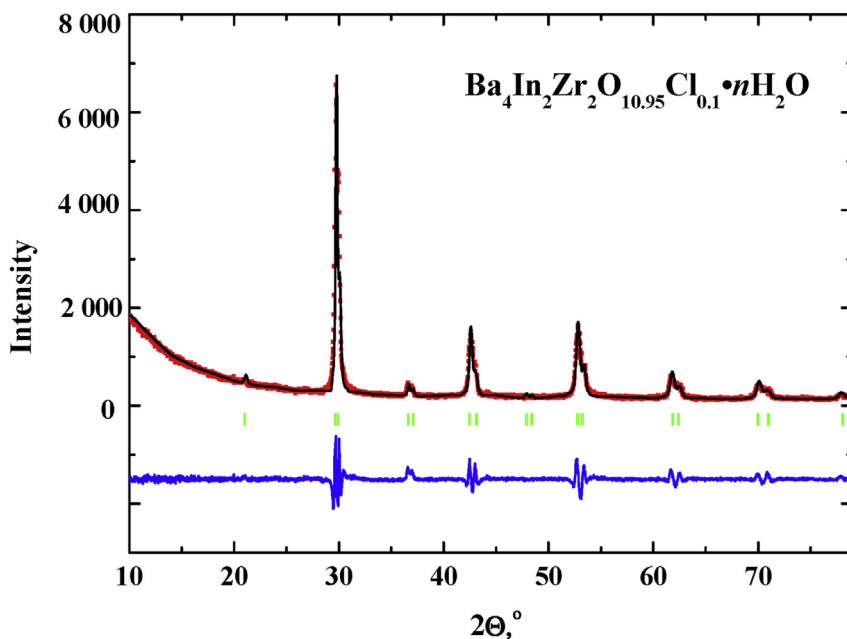


Fig. 1. TG and MS data for the compositions  $\text{Ba}_2\text{In}_2\text{O}_{4.95}\text{Cl}_{0.1} \cdot n\text{H}_2\text{O}$  (a) and  $\text{Ba}_4\text{In}_2\text{Zr}_2\text{O}_{10.95}\text{Cl}_{0.1} \cdot n\text{H}_2\text{O}$  (b). TG, thermogravimetric.

Table 2

Cell volume of hydrated samples.

Sample	$V(\text{\AA}^3)$	Sample	$V(\text{\AA}^3)$	Sample	$V(\text{\AA}^3)$
$\text{Ba}_2\text{In}_2\text{O}_5$ [16]	156.62	$\text{Ba}_4\text{In}_2\text{Zr}_2\text{O}_{11}$ [17]	75.50	$\text{Ba}_4\text{Ca}_2\text{Nb}_2\text{O}_{11}$ [18]	304.98
$\text{Ba}_2\text{In}_2\text{O}_{4.95}\text{F}_{0.1}$	156.51	$\text{Ba}_4\text{In}_2\text{Zr}_2\text{O}_{10.95}\text{F}_{0.1}$ [14]	75.25	$\text{Ba}_4\text{Ca}_2\text{Nb}_2\text{O}_{10.95}\text{F}_{0.1}$ [15]	615.68
$\text{Ba}_2\text{In}_2\text{O}_{4.95}\text{Cl}_{0.1}$	156.64	$\text{Ba}_4\text{In}_2\text{Zr}_2\text{O}_{10.95}\text{Cl}_{0.1}$	75.69	$\text{Ba}_4\text{Ca}_2\text{Nb}_2\text{O}_{10.95}\text{Cl}_{0.1}$	615.72



**Fig. 2.** XRD patterns of  $\text{Ba}_4\text{In}_2\text{Zr}_2\text{O}_{10.95}\text{Cl}_{0.1}\cdot n\text{H}_2\text{O}$ . At the bottom of the figure, the pattern is the difference between the experimental and the calculated one after refinement. Vertical bars show the Bragg angle positions.

carried out. The  $\text{CO}_2/\text{air}$  (1:1) mixture at  $500^\circ\text{C}$  for 10 hours was used. Fig. 3 shows the XRD patterns for powder samples after this treatment. As can be seen, no secondary phases can be observed for  $\text{Ba}_2\text{In}_2\text{O}_{4.95}\text{X}_{0.1}$ ,  $\text{Ba}_4\text{In}_2\text{Zr}_2\text{O}_{10.95}\text{X}_{0.1}$ , and  $\text{Ba}_4\text{Ca}_2\text{Nb}_2\text{O}_{10.95}\text{X}_{0.1}$  samples. They retain their structure without detectable impurities. On the contrary, undoped compounds  $\text{Ba}_2\text{In}_2\text{O}_5$ ,  $\text{Ba}_4\text{In}_2\text{Zr}_2\text{O}_{11}$ , and  $\text{Ba}_4\text{Ca}_2\text{Nb}_2\text{O}_{11}$  decompose in  $\text{CO}_2/\text{air}$  atmosphere according to the following chemical equations:

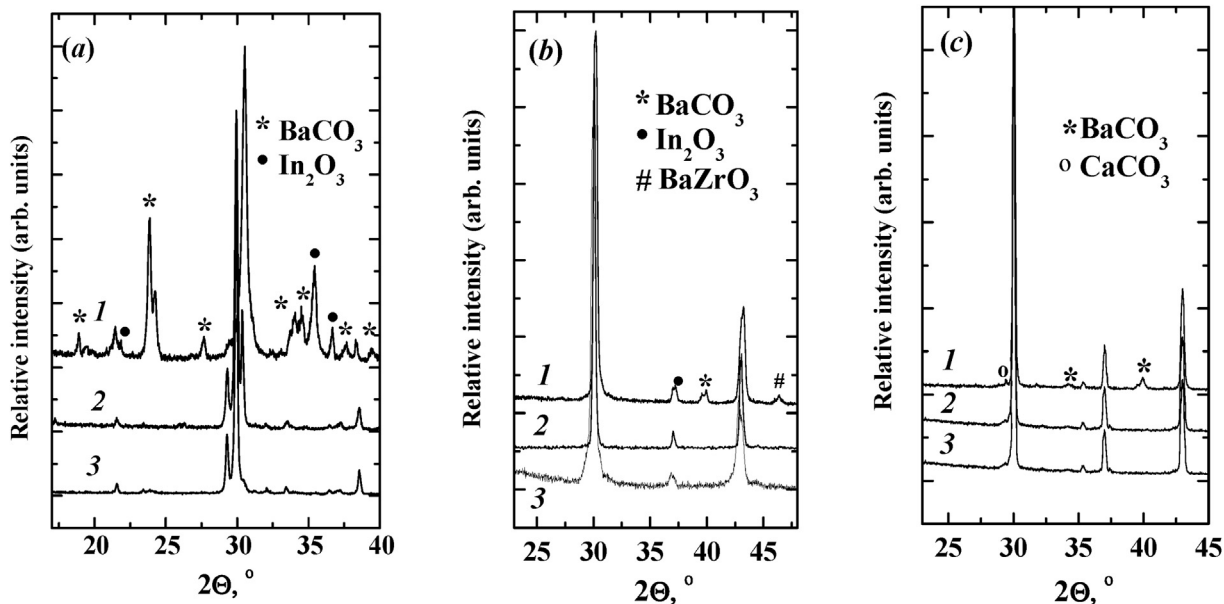
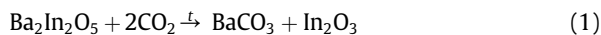
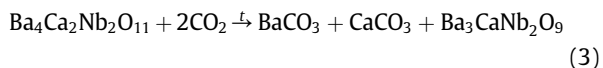


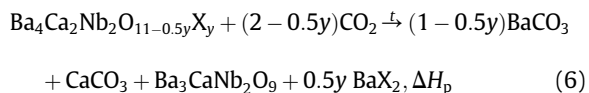
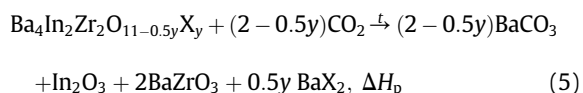
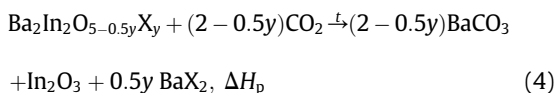
**Fig. 3.** XRD patterns of (a)  $\text{Ba}_2\text{In}_2\text{O}_5$  (1),  $\text{Ba}_2\text{In}_2\text{O}_{4.95}\text{F}_{0.1}$  (2), and  $\text{Ba}_2\text{In}_2\text{O}_{4.95}\text{Cl}_{0.1}$  (3); (b)  $\text{Ba}_4\text{In}_2\text{Zr}_2\text{O}_{11}$  (1),  $\text{Ba}_4\text{In}_2\text{Zr}_2\text{O}_{10.95}\text{F}_{0.1}$  (2), and  $\text{Ba}_4\text{In}_2\text{Zr}_2\text{O}_{10.95}\text{Cl}_{0.1}$  (3); and (c)  $\text{Ba}_4\text{Ca}_2\text{Nb}_2\text{O}_{11}$  (1),  $\text{Ba}_4\text{Ca}_2\text{Nb}_2\text{O}_{10.95}\text{F}_{0.1}$  (2),  $\text{Ba}_4\text{Ca}_2\text{Nb}_2\text{O}_{10.95}\text{Cl}_{0.1}$  and (3) after treatment in a mixture of  $\text{CO}_2/\text{air}$  1:1 at  $500^\circ\text{C}$  for 10 hours



On the basis of the obtained XRD patterns (peak height), the approximate calculations (under the neglect of corundum numbers) of the impurity content in decomposed samples were made. The total impurity content in the samples  $\text{Ba}_2\text{In}_2\text{O}_5$ ,  $\text{Ba}_4\text{In}_2\text{Zr}_2\text{O}_{11}$ , and  $\text{Ba}_4\text{Ca}_2\text{Nb}_2\text{O}_{11}$  after  $\text{CO}_2$  treatment was 40%, 12%, and 8%, respectively.

It is clear that doped compositions are chemically more stable than undoped  $\text{Ba}_2\text{In}_2\text{O}_5$ ,  $\text{Ba}_4\text{In}_2\text{Zr}_2\text{O}_{11}$ , and  $\text{Ba}_4\text{Ca}_2\text{Nb}_2\text{O}_{11}$ ; thus, the introduction of  $\text{F}^-$  and  $\text{Cl}^-$  ions in the oxygen sublattice is a promising method for improving the chemical stability of complex oxides. To explain this fact, the thermodynamic stability of oxygen-deficient complex oxides during anion doping was evaluated.

As it is well known, the evaluation criterion for the possibility of happening of the chemical process is the value of the change in Gibbs free energy  $\Delta G_p$  or the value of the enthalpy  $\Delta H_p$ :



Because the value of  $\Delta H_p$  is defined as the difference between of the enthalpies of formation  $\Delta H_f$  of the reaction products and of  $\Delta H_f$  of the starting materials, it is obvious that the smaller  $\Delta H_f$  of the first and the larger of the second leads to the greater of the  $\Delta H_p$ , and, consequently, to the decrease in the preference of this reaction.

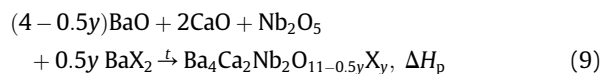
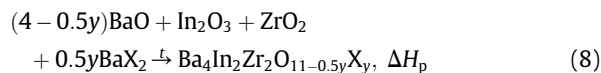
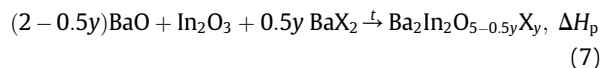
The thermodynamic stability is associated with the enthalpy of formation of the substance. The change in the enthalpy of formation of solid solutions from the starting

**Table 3**

Tolerance factors and average-weighted anion radius for halide-doped solid solutions based on  $\text{Ba}_2\text{In}_2\text{O}_5$ ,  $\text{Ba}_4\text{In}_2\text{Zr}_2\text{O}_{11}$ , and  $\text{Ba}_4\text{Ca}_2\text{Nb}_2\text{O}_{11}$ .

Sample	Average-weighted ionic radius (Å)	Tolerance factor (t)
$\text{Ba}_2\text{In}_2\text{O}_5$	1.40 [4]	0.96(745)
$\text{Ba}_2\text{In}_2\text{O}_{4.95}\text{F}_{0.1}$	1.3986	0.96(762)
$\text{Ba}_2\text{In}_2\text{O}_{4.95}\text{Cl}_{0.1}$	1.4081	0.96(648)
$\text{Ba}_4\text{In}_2\text{Zr}_2\text{O}_{11}$	1.40 [4]	0.98(536)
$\text{Ba}_4\text{In}_2\text{Zr}_2\text{O}_{10.95}\text{F}_{0.1}$	1.3994	0.98(544)
$\text{Ba}_4\text{In}_2\text{Zr}_2\text{O}_{10.95}\text{Cl}_{0.1}$	1.4037	0.98(489)
$\text{Ba}_4\text{Ca}_2\text{Nb}_2\text{O}_{11}$	1.40 [4]	0.99(829)
$\text{Ba}_4\text{Ca}_2\text{Nb}_2\text{O}_{10.95}\text{F}_{0.1}$	1.3994	0.99(833)
$\text{Ba}_4\text{Ca}_2\text{Nb}_2\text{O}_{10.95}\text{Cl}_{0.1}$	1.4037	0.99(784)

materials (oxides and halides) can be calculated according to the equations:



It is known, that for perovskites the enthalpy of formation of a complex oxide from simple ones is related to the tolerance factor ( $t$ ) [22]. After the calculation of this parameter, it is possible to estimate the changes in the enthalpy of formation for the doped samples compared with undoped samples. In general, for the perovskites  $\text{ABO}_3$  and perovskite-related structures ( $\text{Ba}_2\text{In}_2\text{O}_5$ ) the tolerance factor is calculated as

$$t = \frac{(r_{\text{O}} + r_{\text{A}})}{\sqrt{2}(r_{\text{O}} + r_{\text{B}'})} \quad (10)$$

In the case of the presence of two cations in the B-sublattice of complex oxide with the perovskite structure ( $\text{Ba}_4\text{In}_2\text{Zr}_2\text{O}_{11}$ ), the tolerance factor is calculated as

$$t = \frac{(r_{\text{O}} + r_{\text{A}})}{\sqrt{2}(r_{\text{O}} + \frac{1}{2}r_{\text{B}'}) + \frac{1}{2}r_{\text{B}''})} \quad (11)$$

For the complex oxides with a double perovskite structure ( $\text{Ba}_4\text{Ca}_2\text{Nb}_2\text{O}_{11}$ ) the tolerance factor can be calculated as

$$t = \sqrt{\frac{(r_{\text{A}} + r_{\text{O}})^2}{\frac{1}{2}(r_{\text{B}'} + r_{\text{B}''} + 2r_{\text{O}})^2} + \frac{1}{4}(r_{\text{B}'} - r_{\text{B}''})^2} \quad (12)$$

The obtained values of the tolerance factor are represented in Table 3. For the calculations the weighted average radius of the anion was used, which is also given in Table 3. Because of the proximity of the values of the tolerance factor for isostructural compositions it can be assumed that the enthalpy  $\Delta H_p$  does not change with the introduction of the dopant.

Then, we can transform the equations for the calculation of  $\Delta H_p$

$$\Delta H_p = \Delta H_f(\text{Ba}_2\text{In}_2\text{O}_{5-0.5y}\text{X}_y) - (2 - 0.5y) \cdot \Delta H_f\text{BaO} - \Delta H_f(\text{In}_2\text{O}_3) - 0.5y \cdot \Delta H_f(\text{BaX}_2) \quad (13)$$

$$\Delta H_p = \Delta H_f(\text{Ba}_4\text{In}_2\text{Zr}_2\text{O}_{11-0.5y}\text{X}_y) - (4-x) \cdot \Delta H_f(\text{BaO}) - \Delta H_f(\text{In}_2\text{O}_3) - \Delta H_f(\text{ZrO}_2) - 0.5y \cdot \Delta H_f(\text{BaX}_2) \quad (14)$$

$$\Delta H_p = \Delta H_f(\text{Ba}_4\text{Ca}_2\text{Nb}_2\text{O}_{11-0.5y}\text{X}_y) - (4-x) \cdot \Delta H_f(\text{BaO}) - 2 \cdot \Delta H_f(\text{CaO}) - \Delta H_f(\text{Nb}_2\text{O}_5) - 0.5y \cdot \Delta H_f(\text{BaX}_2) \quad (15)$$

into the equations for the calculation of the enthalpy of formation of solid solutions  $\Delta H_f$ :

$$\Delta H_f(\text{Ba}_2\text{In}_2\text{O}_{5-0.5y}\text{X}_x) = \Delta H_p + (2-0.5y) \cdot \Delta H_f(\text{BaO}) + \Delta H_f(\text{In}_2\text{O}_3) + 0.5y \cdot \Delta H_f(\text{BaX}_2) \quad (16)$$

$$\Delta H_f(\text{Ba}_4\text{In}_2\text{Zr}_2\text{O}_{11-0.5y}\text{X}_y) = \Delta H_p + (4-0.5y) \cdot \Delta H_f(\text{BaO}) + \Delta H_f(\text{In}_2\text{O}_3) + \Delta H_f(\text{ZrO}_2) + 0.5y \cdot \Delta H_f(\text{BaX}_2) \quad (17)$$

$$\Delta H_f(\text{Ba}_4\text{Ca}_2\text{Nb}_2\text{O}_{11-0.5y}\text{X}_y) = \Delta H_p + (4-0.5y) \cdot \Delta H_f(\text{BaO}) + 2 \cdot \Delta H_f(\text{CaO}) + \Delta H_f(\text{Nb}_2\text{O}_5) + 0.5y \cdot \Delta H_f(\text{BaX}_2) \quad (18)$$

As can be seen, the presence of the halide dopant affects only on the terms  $\Delta H_f(\text{BaO})$  and  $\Delta H_f(\text{BaX}_2)$  (i.e.  $\Delta H_f(\text{BaF}_2)$  and  $\Delta H_f(\text{BaCl}_2)$ ), the amounts of which are  $-538$ ,  $-1192$ ,  $-860$  kJ/mol, respectively. At the halide doping the appearance of term  $\Delta H_f(\text{BaX}_2)$  is more valuable than that of the decrease of term  $\Delta H_f(\text{BaO})$ , which leads to the decrease in the enthalpy of formation of complex oxides and to the increase in their chemical stability.

#### 4. Conclusions

The investigations of chemical stability of halogen-substituted complex oxides based on proton conductors  $\text{Ba}_2\text{In}_2\text{O}_5$ ,  $\text{Ba}_4\text{In}_2\text{Zr}_2\text{O}_{11}$ , and  $\text{Ba}_4\text{Ca}_2\text{Nb}_2\text{O}_{11}$  to water vapor

and carbon dioxide were carried out. It was proved that  $\text{F}^-$  and  $\text{Cl}^-$ -containing samples are more chemically stable compared with undoped compositions. The enthalpy of decomposition becomes less favorable (less exothermic) with the increase in the halide concentration. The method of halide doping can be used as the promising technique for obtaining the new perovskite-related materials with high chemical stability.

#### Acknowledgments

This work was financially supported by the Russian Science Foundation (project 18-73-00006).

#### References

- [1] H. Iwahara, Y. Asakura, K. Katahira, M. Tanaka, *Solid State Ionics* 168 (2004) 299.
- [2] S. Tao, J.T.S. Irvine, *Adv. Mater.* 18 (2006) 1581.
- [3] E. Fabbri, L. Bi, D. Pergolesi, E. Traversa, *Adv. Mater.* 24 (2012) 195.
- [4] P. Colomban, O. Zaafrani, A. Ślodziak, *Membranes* 2 (2012) 493.
- [5] M. Marrony, J. Dailly, *ECS Trans.* 78 (2017) 3349.
- [6] A. Dubois, S. Ricote, R.J. Braun, *ECS Trans.* 78 (2017) 1963.
- [7] E. Shin, M. Shin, H. Lee, J.-S. Park, *Ceram. Int.* 44 (2018) 8423.
- [8] J.H. Shim, *Nat. Energy* 3 (2018) 168.
- [9] P. Pasier, R. Gajerski, M. Osiadly, A. Lacz, *J. Therm. Anal. Calorim.* 117 (2014) 683.
- [10] Y. Wang, H. Wang, T. Liu, F. Chen, C. Xia, *Electrochem. Commun.* 28 (2013) 87.
- [11] H. Zhou, L. Dai, L. Jia, J. Zhu, Y. Li, L. Wang, *Int. J. Hydrogen Energy* 40 (2015) 8980.
- [12] N.A. Tarasova, Y.V. Filinkova, I.E. Animitsa, *Russ. J. Electrochem.* 49 (2013) 45.
- [13] N. Tarasova, I. Animitsa, *Solid State Ionics* 317 (2018) 21.
- [14] N. Tarasova, I. Animitsa, *Solid State Sci.* 87 (2019) 45.
- [15] N.A. Tarasova, I.E. Animitsa, *Russ. J. Electrochem.* 54 (2018) 1104.
- [16] N. Tarasova, P. Colomban, I. Animitsa, *J. Phys. Chem. Solids* 118 (2018) 32.
- [17] R.D. Shannon, *Acta Crystallogr., A.* 32 (1976) 155.
- [18] T. Schöber, J. Friedrich, *Solid State Ionics* 113–115 (1998) 369.
- [19] I.E. Animitsa, E.N. Dogodaeva, S.S. Nokhrin, O.A. Kosareva, A.Y. Neiman, *Synthesis, Russ. J. Electrochem.* 46 (2010) 734.
- [20] I.E. Animitsa, N.A. Kochetova, *Chim. Techno Acta* 1 (2016) 5, <https://doi.org/10.15826/chimtech.2016.3.1.001>.
- [21] N.A. Tarasova, I.E. Animitsa, K.G. Belova, *Bull. Russ. Acad. Sci. Phys.* 81 (2017) 632.
- [22] S.M. Haile, G. Staneff, K.H. Ryu, *J. Mat. Sci.* 36 (2001) 1149.